

Green synthesis of NiO/ZnO nanocomposite using *Vitex negundo* leaf extract for antibacterial and anti-inflammatory activities

A. Hajeera Aseen, V. Gowthami*, P. Jyolsna

Department of Physics, School of Basic Science, Vels Institute of Science Technology and Advanced Studies, Chennai - 600117, Tamilnadu, India.

Submitted on: 16-Aug-2024, Accepted and Published on: 20-Dec-2024

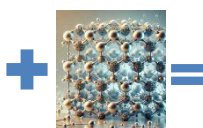
Article

ABSTRACT

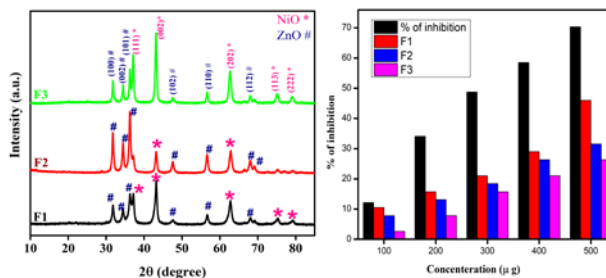
The eco-friendly synthesis of Nickel Oxide/Zinc Oxide (NiO/ZnO) nanocomposite nanoparticles (NPs) using *Vitex negundo* leaf extract offers a sustainable and green approach to developing nanomaterials for biomedical



Vitex Negundo leaves



NiO/ZnO



applications. Three different molar ratios were synthesized: F1 (equal proportion of NiO and ZnO), F2 (high zinc, low nickel), and F3 (high nickel, low zinc). XRD analysis confirmed excellent crystallinity, with ZnO particle sizes of 14.35 nm (F1), 15.91 nm (F2), and 22.97 nm (F3), while NiO sizes ranged from 14.11 nm to 15.75 nm. UV-Vis spectroscopy revealed bandgap energies of 2.7 eV (F1), 2.75 eV (F2), and 2.55 eV (F3), highlighting compositional effects. SEM analysis demonstrated sheets morphology with minimal agglomeration, and EDX confirmed elemental composition. The F1 ratio exhibited superior antibacterial performance, showing a 1.5 mm inhibition zone against *Staphylococcus aureus* and *Pseudomonas aeruginosa*. Anti-inflammatory studies revealed concentration-dependent inhibition, with F1 achieving the highest inhibition (46.2% at 500 µg), though lower than diclofenac (70.3%). This study highlights the successful synthesis of NiO/ZnO nanocomposites, particularly F1, with significant antibacterial and anti-inflammatory potential, emphasizing the role of eco-friendly methods in advancing biomedical research.

Keywords: Green Synthesis, NiO/ZnO Nanocomposite, Vitex Negundo, Antibacterial Activity, Anti-inflammatory Activity

INTRODUCTION

Nanotechnology revolutionizes biomedical applications by enabling precise drug delivery, minimizing side effects, and improving treatment effectiveness.^{1,2} It advances diagnostics with nanoscale biosensors, facilitating early and accurate disease detection. In regenerative medicine, it drives innovations like tissue engineering and nanoparticle-assisted wound healing, expanding the possibilities of modern healthcare.³ Additionally, nanotechnology has become integral to modern scientific research, particularly in developing new materials with unique properties and diverse applications.^{4,5} Among these materials, metal oxide nanoparticles have garnered significant attention for their

exceptional properties, including high surface-to-volume ratio, chemical stability, and multifunctional capabilities. The potential uses of two such metal oxides, Nickel Oxide (NiO) and Zinc Oxide (ZnO), in a variety of sectors, including biomedicine, sensors, electronics, and catalysis, have been extensively investigated.⁶⁻⁸ A variety of applications, such as battery cathodes, supercapacitors, and magnetic storage devices, may utilize the well-known magnetic, catalytic, and electrochemical characteristics of Nickel Oxide nanoparticles.⁹⁻¹³ Antibacterial coatings, medication delivery systems, and sunscreen have all benefited from the exceptional optical, piezoelectric, and antibacterial qualities of Zinc Oxide nanoparticles.¹⁴⁻¹⁸ However, the creation of these nanoparticles frequently uses chemical techniques that might be harmful to the environment because they call for harsh reaction conditions, high temperatures, and toxic solvents. These techniques have the potential to produce hazardous byproducts that threaten both human health and the environment. The ecologically conscious synthesis approach has become a viable and environmentally responsible solution to these challenges. Green synthesis produces nanoparticles in an environmentally safe way by reducing and

*Corresponding Author: Dr. V. Gowthami
Email: gowthamivijayakumar@gmail.com

Cite as: J. Integr. Sci. Technol., 2025, 13(3), 1056.
URN:NBN:sciencein.jist.2025.v13.1056
DOI:10.62110/sciencein.jist.2025.v13.1056



©Authors CC4-NC-ND, ScienceIN <https://pubs.thesciencein.org/jist>

stabilizing metal ions using natural resources like plant extracts.^{19,20} In addition to reducing the amount of hazardous chemicals used, this process gives the produced nanoparticles biocompatibility, which makes them ideal for biological applications^{21,22}. The Chinese chaste tree, or *Vitex Negundo*, is a medicinal plant that has been used for many years in Asian traditional medicine.²³⁻²⁵ *Vitex Negundo*'s leaves are a rich source of flavonoids, terpenoids, glycosides, and alkaloids, among other bioactive substances that support the plant's analgesic, anti-inflammatory, antioxidant, and antibacterial qualities. Due to their phytochemicals' ability to stabilize the produced nanoparticles and decrease metal ions, *Vitex Negundo* is a perfect choice for sustainable synthesis.^{26,27}

In this study focused on the green synthesis of NiO/ZnO nano composed using *Vitex Negundo* leaf extract. The specific nanoparticles lie in the complementary properties of NiO and ZnO, which, when combined, are expected to exhibit enhanced biological activities. The phytochemicals present in *Vitex Negundo* not only facilitate the synthesis of these nanoparticles but also impart additional bioactive properties to the resulting nanocomposites, thereby enhancing their potential for biomedical applications.

The produced NiO/ZnO nanocomposites will be examined by applying a number of scientific approaches, such as Fourier-transform infrared spectroscopy (FT-IR), scanning electron microscopy (SEM), transmission electron microscopy (TEM), and X-ray diffraction (XRD). These methods will provide insights on the compositional, morphological, and physical characteristics of the nanocomposites. The produced nanocomposites' biological activities will also be completely analysed, with a focus on their antibacterial, anti-inflammatory, and antioxidant properties.

Utilizing *Vitex Negundo* leaf extract, the green production of NiO/ZnO nanocomposites offers a fresh method for creating biocompatible materials with improved biological applications. This work is to investigate the possibilities of plant-mediated synthesis in creating cutting-edge materials for medical and environmental applications, as well as to add to the increasing literature of research on sustainable nanotechnology.

EXPERIMENTAL PROCEDURE

Vitex Negundo leaf extract

In order to eliminate any foreign contaminants, fresh *Vitex Negundo* leaves were repeatedly rinsed with purified water. After that, for 30 minutes at 60 °C, 10 g of the finely chopped leaves were mixed with 100 ml of pure water. Filter paper of Whatman No. 1 was then used to filter the leaf extract. Nanoparticle production was carried out using this extract.

Synthesis of NiO/ZnO nano composting nanoparticles

$\text{Ni}(\text{NO}_3)_2 \cdot 6\text{H}_2\text{O}$ and $\text{Zn}(\text{NO}_3)_2 \cdot 6\text{H}_2\text{O}$ salts were used in three distinct molar ratios 1:1, 1:3, and 3:1 to produce nanocomposites: (designated F1, F2, and F3) respectively. By dissolving 2.907 g of NiO and 2.9104 g of ZnO nanoparticles in 100 ml of distilled water to create a 0.1 M solution, NiO/ZnO was created for the F1 nanocomposite. After 20 minutes of constant stirring, the leaf extract was added to this mixture. The nanocomposites were mixed with the leaf extract after 20 minutes, and the mixture was then agitated one more for 30 minutes at 60 °C. To get a gel-like consistency, sodium hydroxide pellets were dissolved in distilled

water and the pH was raised to 10. For three hours, the gel was heated to 100 °C in a hot air oven. A mortar and pestle were used to grind the resultant powder, which was then heated to 500 °C for an hour in a muffle furnace. Further characterization was done using the obtained powder sample. The F2 and F3 nanocomposites followed the same process repeatedly.

XRD characterization

The XRD analysis of the NiO/ZnO nanocomposites synthesized in three different molar ratios (1:1, 1:3, and 3:1) name as F1, F2, and F3. It reveals distinct diffraction patterns corresponding to the crystallographic planes of ZnO and NiO, confirming the formation of these composite nanoparticles. In addition to the structural analysis, the Coulomb interactions between the nanoparticles and the effects on their crystallinity and morphology can be explored to provide a more in-depth understanding of the system.

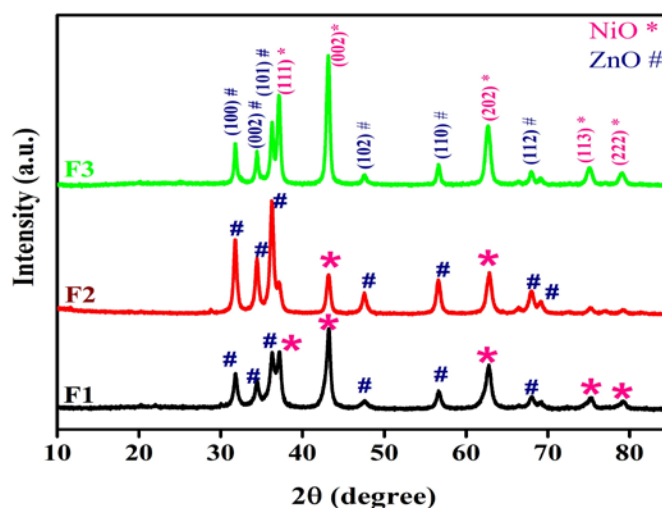


Figure 1. XRD pattern of NiO/ZnO Nanocomposite utilizing the *Vitex Negundo* leaf extract.

The F1 sample diffraction peaks at 2θ values of 37.18°, 43.20°, 62.72°, 75.17°, and 79.12° can be indexed to the (111), (200), (220), (311), and (222) planes of NiO, in line with JCPDS card no. 04-0835, confirming the presence of face-centered cubic NiO²⁹. The diffraction peaks observed at 2θ values of 31.78°, 34.48°, 36.35°, 47.56°, 56.69°, and 67.91° correspond to the (100), (002), (101), (102), (110), and (112) planes of ZnO, following JCPDS card no. 36-1451, indicating that ZnO exhibits a hexagonal wurtzite structure²⁸. The observed peak intensities and sharpness suggest that the electrostatic Coulomb forces between NiO and ZnO facilitate a strong interfacial bonding, preventing significant strain or disorder within the composite is maintaining the distinct crystallographic phases of NiO and ZnO without the formation of secondary phases, as supported by the XRD data.

For the F2 sample, NiO/ZnO nanocomposite, the diffraction peaks at 43.20° and 62.72° match the (200) and (220) planes of face-centered cubic NiO, as per JCPDS card no. 04-0835. The prominent diffraction peaks observed at 31.78°, 34.48°, 36.35°, 47.56°, 56.69°, 67.91°, and 69.15° are indexed to the (100), (002), (101), (102), (110), (112), and (201) planes of ZnO, as indicated by JCPDS card no. 36-1451, confirming the hexagonal wurtzite

structure. The increased ratio of ZnO may lead to stronger Coulombic interactions between the Zn^{2+} and O^{2-} ions compared to the NiO phase, slightly affecting the lattice parameters, as evidenced by minor shifts in the peak positions. These shifts are indicative of the strain that arises from the Coulombic attraction between the different ionic species, which affects the overall lattice structure.

F3 sample nanocomposite, peaks at 37.18° , 43.20° , 62.72° , 75.17° , and 79.12° correspond to the face-centered cubic phase of NiO (JCPDS card no. 04-0835). Additional diffraction peaks at 31.78° , 34.48° , 36.35° , 47.56° , 56.69° , and 67.91° align with the hexagonal wurtzite structure of ZnO (JCPDS card no. 36-1451). Here, the dominance of NiO over ZnO suggests that Coulomb interactions between Ni^{2+} and O^{2-} ions might contribute more significantly to the stabilization of the NiO phase. These electrostatic forces help maintain the integrity of the face-centered cubic structure, as indicated by the absence of secondary phases or impurities in the XRD pattern. The particle size of ZnO and NiO Nano compositing nanoparticles was determined using the Debye-Scherrer equation,

$$D = \frac{k\lambda}{\beta \cos \theta} \quad (1)$$

where D, K, and λ represent the crystal size, Shape factor, and wavelength of the X-ray. β and θ represent the full width at half maximum intensity of the peak and diffraction angle. And also calculated the lattice constant 'a' using the below formula,

$$a = d_{hkl} (h^2 + k^2 + l^2)^{1/2} \quad (2)$$

The NiO particle sizes for the F1, F2, and F3 samples show 14.11 nm, 14.64 nm, and 15.75 nm, respectively. Similarly, the ZnO particle sizes for the F1, F2, and F3 samples show 14.35 nm, 15.91 nm, and 22.97 nm, respectively. These results indicate a trend of increasing particle size with changes in the compositional ratios. Calculated particle sizes, interplanar distances, and lattice constants of the NiO/ZnO Nano compositing NPs are different ratios (F1, F2 and F3) are shown in Tables 1, 2, and 3.

Table 1. Particle size, lattice constant, and interplanar distance of NiO/ZnO Nanocompositing NPs at F1 sample were calculated.

2 θ	hkl	FWHM (β)	d-spacing (\AA)		Crystal size (D)	Lattice constant (a)
			Observed	Calculated		
31.78	100	0.492	2.81	2.81	16.78	2.81
34.48	002	0.539	2.60	2.60	15.42	3.67
36.35	101	0.656	2.47	2.47	12.74	3.49
37.18	101	0.573	2.42	2.42	14.62	3.42
43.2	200	0.474	2.09	2.09	18.01	2.95
47.56	102	0.89	1.90	1.90	9.750	3.29
56.69	110	0.576	1.62	1.62	15.66	2.29
62.72	220	0.69	1.48	1.48	13.47	2.96
67.91	112	0.63	1.37	1.37	15.19	2.74
75.91	311	0.71	1.26	1.26	14.18	2.81
79.12	222	0.96	1.20	1.20	10.72	2.93

FTIR characterization

The FTIR analysis of the NiO/ZnO nanocomposite nanoparticles synthesized using *Vitex Negundo* leaf extract reveals key functional groups involved in their formation and stabilization. The broad

Table 2. Particle size, lattice constant, and interplanar distance of NiO/ZnO Nanocompositing NPs at F2 sample were calculated.

2 θ	hkl	FWHM (β)	d-spacing (\AA)		Crystal size (D)	Lattice constant (a)
			Observed	Calculated		
31.78	100	0.453	2.81	2.81	18.22	2.81
34.48	002	0.466	2.60	2.60	17.00	3.67
36.35	101	0.489	2.47	2.47	17.09	3.49
43.2	200	0.532	2.09	2.09	16.05	2.95
47.56	102	0.600	1.91	1.91	14.46	3.30
56.69	110	0.558	1.62	1.62	16.17	2.29
62.72	220	0.702	1.47	1.47	13.24	2.94
67.91	112	0.653	1.37	1.37	14.66	2.74
69.15	201	0.70	1.35	1.35	13.77	2.33

Table 3. Particle size, lattice constant, and interplanar distance of NiO/ZnO Nanocompositing NPs at F3 sample were calculated.

2 θ	hkl	FWHM (β)	d-spacing (\AA)		Crystal size (D)	Lattice constant (a)
			Observed	Calculated		
31.78	100	0.319	2.81	2.81	25.88	2.81
34.48	002	0.336	2.60	2.60	24.74	3.67
36.35	101	0.364	2.47	2.47	22.96	3.49
37.18	101	0.432	2.42	2.42	19.39	3.42
43.2	200	0.461	2.09	2.09	18.52	2.95
47.56	102	0.43	1.91	1.91	20.18	3.30
56.69	110	0.387	1.62	1.62	23.31	2.29
62.72	220	0.681	1.48	1.48	13.65	2.96
67.91	112	0.461	1.37	1.37	20.76	2.74
75.17	311	0.715	1.26	1.26	14.01	2.81
79.12	222	0.78	1.21	1.21	13.20	2.96

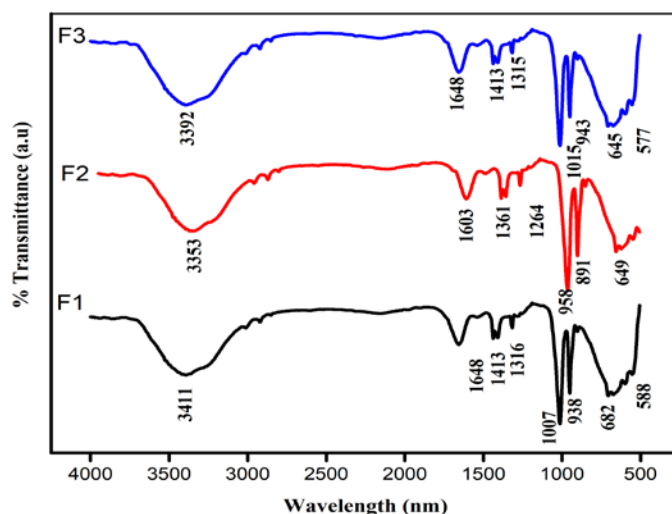


Figure 2. FTIR spectrum of NiO/ZnO Nanocomposite NPs using *Vitex Negundo* leaf extract.

peak observed in the $3353\text{--}3411\text{ cm}^{-1}$ range corresponds to O-H stretching, indicating the presence of hydroxyl groups from biomolecules in the extract.²⁸ Peaks at $1603\text{--}1648\text{ cm}^{-1}$ are recognized to O-H bending vibrations³⁰. Vibrations between 1007 and 1264 cm^{-1} and $1315\text{--}1361\text{ cm}^{-1}$ are indicative of C-H and C=O groups, respectively, and validate the organic capping of nanoparticles.³¹ By confirming the production of Ni-O and Zn-O

bonds, the distinctive metal-oxygen stretching vibrations at $577\text{-}682\text{ cm}^{-1}$ validate the successful synthesis of the nanocomposites.²⁸

UV Characterization

The NiO/ZnO nanocomposites (F1, F2, and F3) exhibited significant absorption in the UV-visible region, with absorption peaks shifting to longer wavelengths when the NiO: ZnO molar ratio varies, according to their UV-Vis absorption spectra, which were recorded within the wavelength range of 300 nm to 800 nm. Strong absorption is seen in the F1 ratio, indicating an equal percentage of NiO and ZnO, however the optical characteristics of F2 and F3, which have different compositional ratios, are dependent on the proportions of NiO and ZnO. ZnO's conduction band electrons and the localized d-electrons of Ni²⁺ ions interact through sp-d exchange interactions, which is reflected in the red shift in the absorption band edge across F1, F2, and F3^{32,33}. This interaction findings in a reduced bandgap energy as the proportion of NiO increases. The bandgap energy (E_g) can be established using the Tauc equation:

$$(\alpha h\nu)^{1/n} = A (h\nu - E_g) \quad (3)$$

Table 4. Shows the wavelength and bandgap energy

NiO/ZnO NPs	Wavelength (nm)	Bandgap Energy (E_g)
F1 ratio	375 nm	2.7 eV
F2 ratio	382 nm	2.75 eV
F3 ratio	391 nm	2.55 eV

When NiO and ZnO are present in similar proportions, the F1 ratio shows a balanced optical response. In contrast to the F3 ratio, which exhibits the lowest bandgap and the most improved optical qualities, the F2 ratio has a little greater bandgap, suggesting less optical activity. These modifications demonstrate how NiO/ZnO nanocomposites' optical characteristics may be tuned, which makes them appropriate for photocatalytic and optoelectronic applications.³⁴

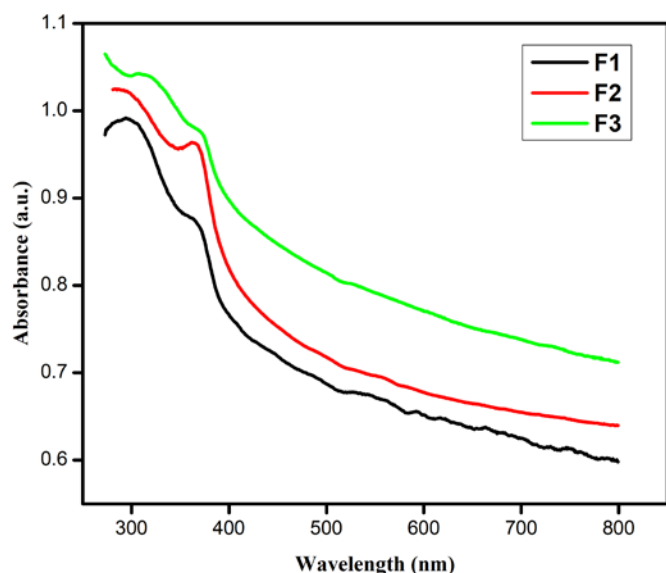


Figure 3. UV Absorption spectrum of NiO/ZnO nanocomposite NPs using *Vitex Negundo* leaf extract.

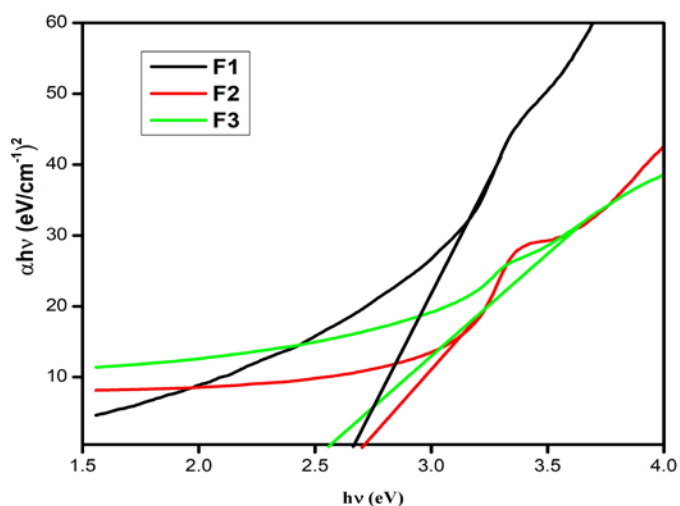


Figure 4. UV Energy bandgap of NiO/ZnO nanocomposite NPs using *Vitex Negundo* leaf extract.

SEM characterization

Well-defined morphological features with agglomerated structures are shown by the SEM analysis of NiO/ZnO nanocomposites made with *Vitex Negundo* leaf extract in an equal ratio. The tightly packed, irregularly shaped nanoparticles at higher magnifications indicate strong contacts between the NiO and ZnO phases. The rough surface shape is probably due to the *Vitex Negundo* extract's function as a capping and reducing agent, which made the composite easier to form. A tendency for aggregation is reflected in the observed particle clusters, which may increase the composite's potential for photocatalytic and biological applications. Overall, the SEM examination validates the green synthesis of NiO/ZnO nanocomposites with consistent surface characteristics and efficient phase interaction.³⁵

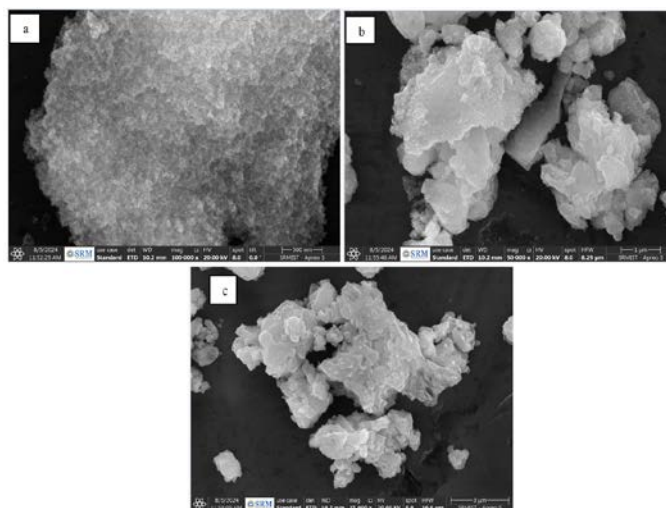


Figure 5. SEM characterization of F1 ratio, NiO/ZnO nanocomposite NPs using *Vitex Negundo* leaf extract.

Different morphological features are revealed by the SEM characterisation of NiO/ZnO nanocomposites made with *Vitex Negundo* leaf extract and a greater nickel to zinc ratio. High

magnification (Figure a) reveals layered and sheet-like structures, which show that NiO predominates while ZnO partially integrates. Figure b at intermediate magnification shows irregular and aggregated particles, suggesting strong interaction and effective bonding between the NiO and ZnO phases. Figure c at lower magnification highlights the overall uniform distribution of the composite with clustered and rough surface features, which could enhance catalytic or biological activity. These observations confirm the successful formation of NiO/ZnO nanocomposites with unique structural characteristics facilitated by the green synthesis method.³⁶

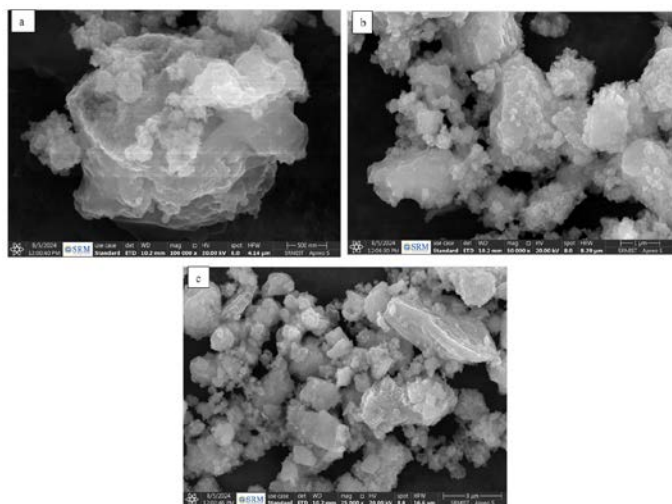


Figure 6. SEM characterization of F2 ratio, NiO/ZnO nanocomposite NPs using *Vitex Negundo* leaf extract.

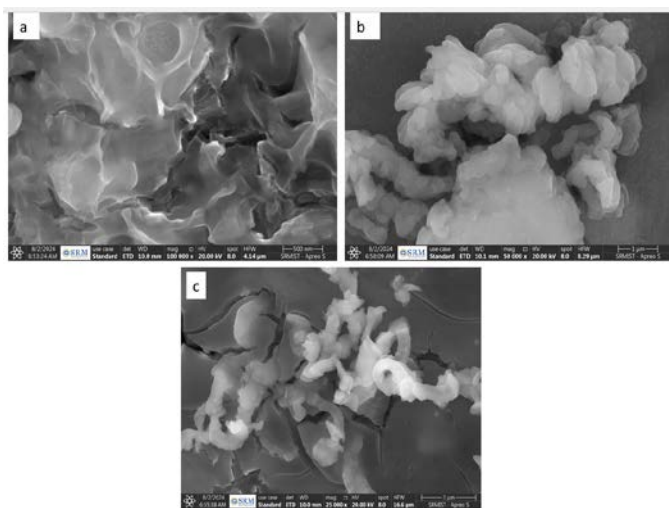


Figure 7. SEM characterization of F3 ratio, NiO/ZnO nanocomposite NPs using *Vitex Negundo* leaf extract.

The SEM characterization of NiO/ZnO nanocomposites synthesized using *Vitex Negundo* leaf extract with an F3 ratio reveals distinct morphological features. At high magnification (Figure a), sheet-like and wrinkled structures are observed, indicating the dominant presence of NiO with minimal ZnO incorporation. (Figure b) at intermediate magnification shows

aggregated and clustered formations, suggesting strong interaction and partial dispersion of ZnO within the NiO matrix. (Figure c) at lower magnification highlights elongated, rough surface textures, reflecting the influence of NiO higher content in shaping the overall morphology. These observations confirm the successful synthesis of NiO/ZnO nanocomposites with hierarchical structural characteristics, achieved through the green synthesis method.

Biological Application

Antibacterial Activity

The antibacterial activity of NiO/ZnO nanocomposites synthesized using *Vitex Negundo* (VN) leaf extract highlights the dual role of the extract as both a reducing and stabilizing agent during the green synthesis process. The VN leaf extract contributed bioactive phytochemicals that may synergize with the nanocomposite's properties, enhancing their biological activity³⁷. The production of reactive oxygen species (ROS) such as hydroxyl radicals (OH) and superoxide anions (O₂⁻) during interactions between the nanocomposites and bacterial cells is the main explanation for the antibacterial mechanism of NiO/ZnO nanocomposites. These ROS induce oxidative stress, which damages DNA, breaks down proteins, and destroys bacterial cell membranes, ultimately leading to bacterial cell death³⁸. Still, the nanocomposites' high surface area and tiny size allow them to more easily enter bacterial cells, improving their bactericidal efficacy.³⁹

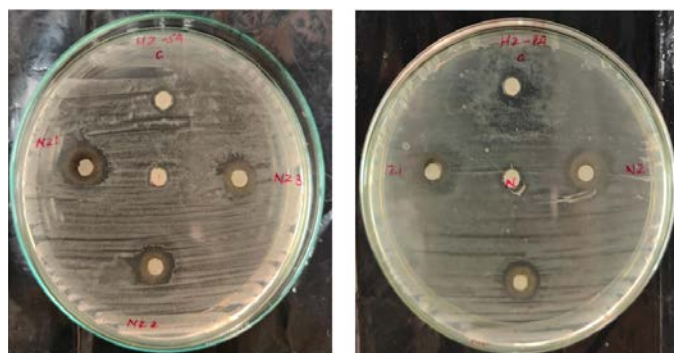


Figure 8. Antibacterial Activity of NiO/ZnO nanocomposting NPs using *Vitex Negundo* leaf extract.

Among the studied ratios (F1, F2, and F3), F1 showed the strongest antibacterial activity, displaying the largest inhibition zones against *Pseudomonas aeruginosa* (1.5 cm) and *Staphylococcus aureus* (1.5 cm). The lowest activity was observed by F3, which produced zones of 0.8 cm and 0.7 cm, whereas F2 had moderate activity with inhibition zones of 1.3 cm and 1.1 cm, respectively. The results were reliable because the control showed no growth and the negative control, DMSO, had no bactericidal effect.

The results highlight the significance of the NiO to ZnO ratio in assessing the nanocomposites' antibacterial efficacy. When combined with the bioactive ingredients in the VN leaf extract, the synergistic action of NiO and ZnO nanoparticles increases ROS production and membrane disruption, which improves antibacterial activity. In addition to lessening the products' negative effects on the environment, this ecologically friendly synthesis method with

VN leaf extract gives the materials a high degree of bioactivity, which makes them desirable choices for antibacterial applications.

Table 5. The antibacterial activity is displayed in the table

Microorganism	DMSO	Control	F1 ratio	F2 ratio	F3 ratio
<i>Staphylococcus aureus</i>	00	1.2	1.5	1.3	0.8
<i>Pseudomonas aeruginosa</i>	00	0.7	1.5	1.1	0.7

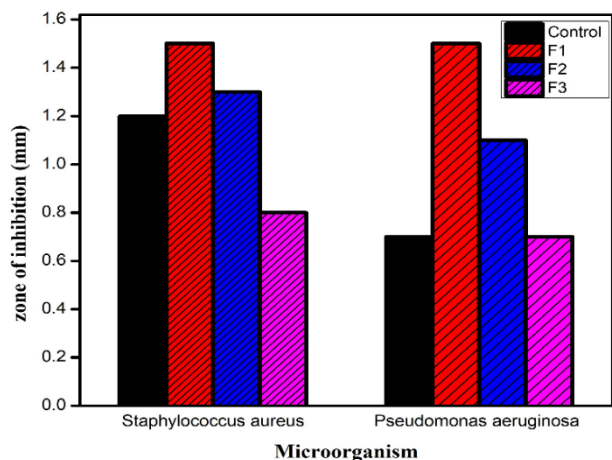


Figure 9. The bar graph shows the Antibacterial Activity of NiO/ZnO nanocomposting NPs using *Vitex Negundo* leaf extract.

Anti-inflammatory activity

The human red blood cell (HRBC) membrane stabilization experiment was used to assess the anti-inflammatory properties of NiO/ZnO nanocomposite nanoparticles made with *Vitex Negundo* leaf extract. With the highest suppression of RBC hemolysis, the F1 ratio (equal parts NiO and ZnO) had superior membrane stability and anti-inflammatory capability, according to the data, which showed a concentration-dependent effect. By contrast, the F3 ratio

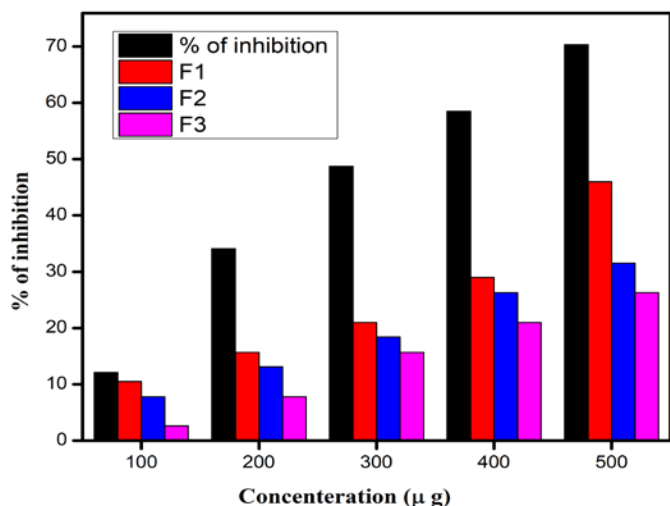


Figure 10. The bar graph shows the Anti-inflammatory activity of NiO/ZnO nanocomposting NPs utilizing *Vitex Negundo* leaf extract.

(high NiO, low ZnO) exhibited the least activity, whilst the F2 ratio (high ZnO, low NiO) displayed moderation. Hemolysis brought on by an excessive buildup of fluid causes membrane rupture and oxidative damage in hypotonic solutions. By stabilizing the RBC membrane, the nanocomposites may be able to stop the release of lytic enzymes and inflammatory mediators, which would lower membrane permeability and the inflammatory reactions that follow. *Vitex Negundo* leaf extract played a crucial role as a green synthesis agent and a source of bioactive substances including flavonoids, which have antioxidant and anti-inflammatory effects. These results demonstrate the potential of environmentally friendly synthetic nanocomposites for applications in medicine and emphasize the importance of the NiO: ZnO ratio in regulating anti-inflammatory activity.^{40,41}

Table 6. Shows the Anti-inflammatory activity

Sample Concentration (µg)	100	200	300	400	500	B
Diclofenac	0.36	0.27	0.21	0.17	0.12	0.41
% of inhibition	12.1	34.1	48.7	58.5	70.3	
F1	0.34	0.32	0.30	0.27	25	0.38
% of inhibition	10.5	15.7	21	28.9	46.2	
F2	0.35	0.33	0.31	0.28	26	
% of inhibition	7.8	13.1	18.4	26.3	31.5	
F3	0.37	0.35	0.32	0.30	28	
% of inhibition	2.63	7.8	15.7	21	26.3	

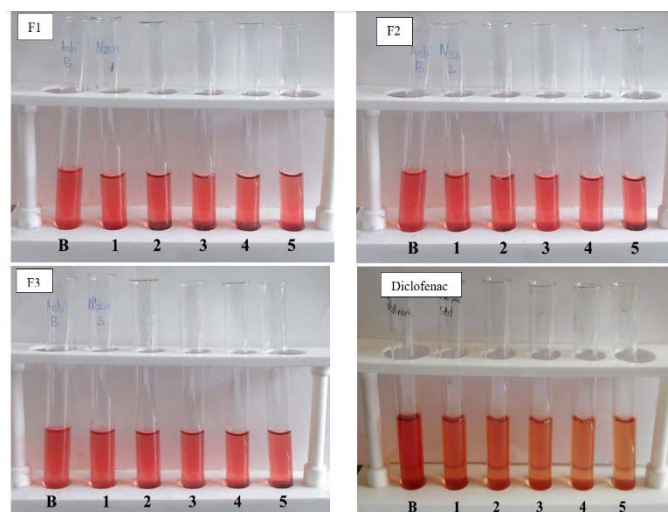


Figure 11. Anti-inflammatory human red blood assay.

CONCLUSION

This work effectively illustrates the environmentally friendly production of NiO/ZnO nanocomposites utilizing leaf extract from *Vitex negundo*, offering a sustainable method for creating useful nanomaterials. The synthesized nanocomposites' outstanding crystallinity was validated by structural analysis, which further highlighted the impact of compositional modifications by seeing significant fluctuations in particle size and bandgap energies across the F1, F2, and F3 ratios. Equal amounts of NiO and ZnO in the F1 ratio made it the most promising formulation. It showed strong

antibacterial activity against *Pseudomonas aeruginosa* and *Staphylococcus aureus*, as well as significant anti-inflammatory benefits, albeit they were not as strong as those of the common medication diclofenac. The findings highlight the promise of NiO/ZnO nanocomposites produced by green synthesis for use in biomedical applications, specifically in antibacterial and anti-inflammatory treatments. By utilizing their environmental sustainability, these results open the door for additional study into environmentally friendly nanomaterials.

CONFLICT OF INTEREST STATEMENT

Authors declare that there is no conflict of interest regarding the publication of this paper.

REFERENCES AND NOTES

- S. Malik, K. Muhammad, Y. Waheed. Nanotechnology: A Revolution in Modern Industry. *Molecules* **2023**, 28 (2), 661.
- A.R. Dhanapal, M. Thiruvengadam, J. Vairavanathan, et al. Nanotechnology Approaches for the Remediation of Agricultural Polluted Soils. *ACS Omega* **2024**, 9 (12), 13522–13533.
- C. Chen, L. Berglund, I. Burgert, L. Hu. Wood Nanomaterials and Nanotechnologies. *Adv. Mater.* **2021**, 33 (28), 2006207.
- Q. Huang, Y. Chen, W. Zhang, et al. Nanotechnology for enhanced nose-to-brain drug delivery in treating neurological diseases. *J. Control. Release* **2024**, 366, 519–534.
- A.P. Ramos, M.A.E. Cruz, C.B. Tovani, P. Ciancaglini. Biomedical applications of nanotechnology. *Biophysical Reviews*. 2017, pp 79–89.
- B.S. Chhikara. Current trends in nanomedicine and nanobiotechnology research. *J. Mater. Nanosci.* **2017**, 4 (1), 19–24.
- P. Kurhade, S. Kodape, R. Choudhury. Overview on green synthesis of metallic nanoparticles. *Chem. Pap.* **2021**, 75 (10), 5187–5222.
- M.S. Chavali, M.P. Nikolova. Metal oxide nanoparticles and their applications in nanotechnology. *SN Appl. Sci.* **2019**, 1 (6), 607.
- A.A. Olajire, A.A. Mohammed. Green synthesis of nickel oxide nanoparticles and studies of their photocatalytic activity in degradation of polyethylene films. *Adv. Powder Technol.* **2020**, 31 (1), 211–218.
- S. Chakrabarty, K. Chatterjee. A facile and general route to size-controlled synthesis of metal (Ni, Co and Mn) oxide nanoparticle and their optical behavior. *Nanosci. Methods* **2012**, 1 (1), 213–222.
- D. Deepthi, B.S. Rahman, M. Senthilkumar, et al. Green synthesis of NiO nanoparticles, phytochemical screening and antibacterial activity of aqueous leaf extract of *Jatropha gossypifolia* (L.). *J. Pharmacogn. Phytochem.* **2021**, 10 (2), 20–28.
- G. Ilbeigi, A. Kariminik, M.H. Moshafi. The Antibacterial Activities of NiO Nanoparticles Against Some Gram-Positive and Gram-Negative Bacterial Strains. *Int. J. Basic Sci. Med.* **2019**, 4 (2), 69–74.
- S.U. Din, H. Iqbal, S. Haq, et al. Investigation of the Biological Applications of Biosynthesized Nickel Oxide Nanoparticles Mediated by *Buxus wallichiana* Extract. *Crystals* **2022**, 12 (2), 146.
- T.S. Aldeen, H.E. Ahmed Mohamed, M. Maaza. ZnO nanoparticles prepared via a green synthesis approach: Physical properties, photocatalytic and antibacterial activity. *J. Phys. Chem. Solids* **2022**, 160, 110313.
- H. Chemingui, T. Missaoui, J.C. Mzali, et al. Facile green synthesis of zinc oxide nanoparticles (ZnO NPs): Antibacterial and photocatalytic activities. *Mater. Res. Express* **2019**, 6 (10), 1050 4.
- M.G. Demissie, F.K. Sabir, G.D. Edossa, B.A. Gonfa. Synthesis of Zinc Oxide Nanoparticles Using Leaf Extract of *Lippia adoensis* (Koseret) and Evaluation of Its Antibacterial Activity. *J. Chem.* **2020**, 2020, 7459042.
- R. Saemi, E. Taghavi, H. Jafarizadeh-Malmiri, N. Anarjan. Fabrication of green ZnO nanoparticles using walnut leaf extract to develop an antibacterial film based on polyethylene-starch-ZnO NPs. *Green Process. Synth.* **2021**, 10 (1), 112–124.
- S.S. Rad, A.M. Sani, S. Mohseni. Biosynthesis, characterization and antimicrobial activities of zinc oxide nanoparticles from leaf extract of *Mentha pulegium* (L.). *Microb. Pathog.* **2019**, 131, 239–245.
- S. Pandit, A.C. Bhowal, S. Kundu. Green synthesis of silver nanoparticles and its potential applications. *Appl. Silver Nanoparticles* **2023**, 38, 41–74.
- F. Khan, M. Shariq, M. Asif, et al. Green Nanotechnology: Plant-Mediated Nanoparticle Synthesis and Application. *Nanomaterials* **2022**, 12 (4), 673.
- T. Mazhar, V. Shrivastava, R.S. Tomar. Green synthesis of bimetallic nanoparticles and its applications: A review. *J. Pharm. Sci. Res.* **2017**, 9 (2), 102–110.
- M.S. Samuel, M. Ravikumar, A. John, et al. A Review on Green Synthesis of Nanoparticles and Their Diverse Biomedical and Environmental Applications. *Catalysts* **2022**, 12 (5), 459.
- M.M. Shanwaz, P. Shyam. Synthesis of Silver Nanoparticles from *Vitex negundo* Plant by Green Method and their Bactericidal Effects. *Lett. Appl. NanoBioScience* **2023**, 12 (2), 59–62.
- B.S. Gill, R. Mehra, Naveet, S. Kumar. *Vitex negundo* and its medicinal value. *Mol. Biol. Rep.* **2018**, 45 (6), 2925–2934.
- P. Karnan, A. Anbarasu, N. Deepa, R. Usha. Green Biosynthesis of Magnetic Iron Oxide Nanoparticles of *Vitex Negundo* Aqueous Extract. *Int. J. Curr. Pharm. Res.* **2018**, 10 (3), 11.
- M.F. Khan, P. Arora, M. Dhobi. A Prospective Review on Phyto-pharmacological Aspects of *Vitex negundo* Linn. *Curr. Tradit. Med.* **2019**, 7 (1), 138–150.
- N. Das, A.C.F. Salgueiro, D.R. Choudhury, et al. Traditional uses, phytochemistry, and pharmacology of genus *Vitex* (Lamiaceae). *Phyther. Res.* **2022**, 36 (2), 571–671.
- M. Hessien, E. Da'na, A. Taha. Phytoextract assisted hydrothermal synthesis of ZnO–NiO nanocomposites using neem leaves extract. *Ceram. Int.* **2021**, 47 (1), 811–816.
- K. Lingaraju, H. Raja Naika, H. Nagabhushana, et al. Biosynthesis of Nickel oxide Nanoparticles from *Euphorbia heterophylla* (L.) and their biological application. *Arab. J. Chem.* **2020**, 13 (3), 4712–4719.
- N.M. Mahmoodi, Z. Hosseinabadi-Farahani, F. Bagherpour, et al. Synthesis of CuO–NiO nanocomposite and dye adsorption modeling using artificial neural network. *Desalin. Water Treat.* **2016**, 57 (37), 17220–17229.
- S. Haq, A.W. Raja, S.U. Rehman, et al. Phyto-genic Synthesis and Characterization of NiO-ZnO Nanocomposite for the Photodegradation of Brilliant Green and 4-Nitrophenol. *J. Chem.* **2021**, 2021.
- S. Deka, P.A. Joy. Direct observation of Ni metal impurities in lightly doped ferromagnetic polycrystalline (ZnNi)O. *Chem. Mater.* **2005**, 17 (26), 6507–6510.
- P. V. Radovanovic, D.R. Gamelin. High-temperature ferromagnetism in [formula presented]-doped zno aggregates prepared from colloidal diluted magnetic semiconductor quantum dots. *Phys. Rev. Lett.* **2003**, 91 (15), 157202.
- S. Thambidurai, P. Gowthaman, M. Venkatachalam, S. Suresh. Enhanced bactericidal performance of nickel oxide-zinc oxide nanocomposites synthesized by facile chemical co-precipitation method. *J. Alloys Compd.* **2020**, 830, 154642.
- M.A. Kanjwal, W.W.F. Leung. Electrospun Nanofibers of p-Type CuO/n-type TZB-Gr Heterojunctions with Enhanced Photocatalytic Activity. *Mater. Chem. Phys.* **2019**, 232, 475–484.
- M. Xiao, Y. Lu, Y. Li, et al. A new type of p-type NiO/n-type ZnO nano-heterojunctions with enhanced photocatalytic activity. *RSC Adv.* **2014**, 4 (65), 34649–34653.
- J.K. Patra, K.H. Baek. Antibacterial activity and synergistic antibacterial potential of biosynthesized silver nanoparticles against foodborne pathogenic bacteria along with its anticandidal and antioxidant effects. *Front. Microbiol.* **2017**, 8 (FEB), 167.
- D. Paul, S. Mangla, S. Neogi. Antibacterial study of CuO-NiO-ZnO trimetallic oxide nanoparticle. *Mater. Lett.* **2020**, 271, 127740.
- P. Yadav, N. Bharti, S.K. Choudhary, R.K. Dhaked, P.C. Mali. Assessment of the antifertility potential of Silver nanoparticles synthesized using *Pongamia pinnata* leaf extract in male wistar rats for the development of a male contraceptive agent. *Biomed. Ther. Lett.* **2024**, 11 (2), 918.
- A.S. Abdelbaky, T.A. Abd El-Mageed, A.O. Babalghith, S. Selim, A.M.H.A. Mohamed. Green Synthesis and Characterization of ZnO Nanoparticles Using *Pelargonium odoratissimum* (L.) Aqueous Leaf Extract and Their Antioxidant, Antibacterial and Anti-inflammatory Activities. *Antioxidants* **2022**, 11 (8), 11.
- P. Lakra, I.N. Gahlawat. Regular food chemicals as antioxidant towards prevention of diseases – An insight review. *J. Mol. Chem.* **2022**, 2 (2), 441.